NRC Publications Archive
Archives des publications du CNRC

Ex situ measurement of strain associated with hot tearing in AZ91D and AE42 magnesium alloys using neutron diffraction

Bichler, L.; Ravindran, C.; Sediako, D.

This publication could be one of several versions: author's original, accepted manuscript or the publisher's version. / La version de cette publication peut être l'une des suivantes : la version prépublication de l'auteur, la version acceptée du manuscrit ou la version de l'éditeur.
For the publisher's version, please access the DOI link below./ Pour consulter la version de l'éditeur, utilisez le lien DOI ci-dessous.

Publisher's version / Version de l'éditeur:
https://doi.org/10.1139/P09-106
Canadian Journal of Physics, 88, 10, pp. 715-721, 2010-04-30

NRC Publications Record / Notice d'Archives des publications de CNRC:
https://nrc-publications.canada.ca/eng/view/object/?id=5809ec7f-2473-4f9f-af3f-a95089a7b21f
https://publications-cnrc.canada.ca/fra/voir/objet/?id=5809ec7f-2473-4f9f-af3f-a95089a7b21f

Access and use of this website and the material on it are subject to the Terms and Conditions set forth at
https://nrc-publications.canada.ca/eng/copyright
READ THESE TERMS AND CONDITIONS CAREFULLY BEFORE USING THIS WEBSITE.

L'accès à ce site Web et l'utilisation de son contenu sont assujettis aux conditions présentées dans le site
https://publications-cnrc.canada.ca/fra/droits
LISEZ CES CONDITIONS ATTENTIVEMENT AVANT D'UTILISER CE SITE WEB.

Questions? Contact the NRC Publications Archive team at
PublicationsArchive-ArchivesPublications@nrc-cnrc.gc.ca. If you wish to email the authors directly, please see the first page of the publication for their contact information.

Vous avez des questions? Nous pouvons vous aider. Pour communiquer directement avec un auteur, consultez la première page de la revue dans laquelle son article a été publié afin de trouver ses coordonnées. Si vous n'arrivez pas à les repérer, communiquez avec nous à PublicationsArchive-ArchivesPublications@nrc-cnrc.gc.ca.

National Research Council Canada   Conseil national de recherches Canada

Ex situ measurement of strain associated with hot tearing in AZ91D and AE42 magnesium alloys using neutron diffraction [1]

L. Bichler, C. Ravindran, and D. Sediako

Abstract: Prevention of hot tearing during casting or welding of commercial alloys remains a challenge for numerous industrial applications. The tendency of an alloy to tear is related to the alloy's microstructure, solidification rate, and the stress/strain conditions it experiences during solidification. Due to technological challenges in performing accurate and reliable measurements, there remains a paucity of quantitative experimental data on the stress/strain conditions associated with the onset of hot hearing. This paper reports on a novel approach to quantify strain at the onset of hot tearing in two magnesium alloys. Neutron diffraction strain mapping was carried out and revealed that in the case of the AZ91D alloy, tensile strain of $\sim 0.05\%$ was associated with initiation of material's plastic damage and hot tearing, while for the AE42 alloy the critical strain was $\sim 0.09\%$.

PACS No: 61.05.fg

Résumé : La prévention de la fissuration à chaud lors de la coulée ou du soudage d'alliages métalliques demeure un défi dans beaucoup d'applications industrielles. La tendance d'un alliage à se déchirer est reliée à la microstructure de l'alliage, au taux de solidification et aux conditions de contrainte et de déformation pendant la solidification. À cause des limitations technologiques actuelles, il est difficile d'obtenir des mesures précises et fiables des conditions de contrainte et déformation associées au début de la fissuration à chaud. Nous présentons ici une nouvelle approche pour quantifier la déformation au début de la fissuration à chaud dans deux alliages de magnésium. Une cartographie des déformations, obtenue par diffraction de neutrons, révèle que dans le cas de l'alliage AZ91D, une déformation sous traction de $\sim 0{,}05$ % est associée au début du dommage plastique et de la fissuration à chaud, alors que pour l'alliage AE42, la déformation critique est de $\sim 0{,}09$ %.

[Traduit par la Rédaction]

1. Introduction

Hot tears are cracks forming in a semi-solid alloy prior to its complete solidification. These cracks may be observed on the casting surface or in the casting interior [1]. Hot tearing has been observed in many engineering materials including steels, aluminum and magnesium alloys. Hot tears form when a casting is in a semi-solid state and experiences significant thermal and mechanical tensile stresses. Thermal stresses result from a non-uniform temperature distribution leading to non-uniform solidification shrinkage and thermal contraction of a casting upon solidification. Mechanical stresses develop when a casting solidifies within a rigid mold, which limits the casting's solidification shrinkage and thermal contraction.

Reviews of hot tearing theories, evaluation methods, and predictive models based on empirical evidence are available in the literature [2–5]. These and other research investigations identified stress/strain, alloy microstructure, and solidification of a given alloy as the key parameters affecting the onset of hot tearing. Theoretical criterion functions based on these three parameters were developed with the aim of predicting the onset of hot tearing [6]. Quantification of alloy microstructure and solidification history attained high levels of sophistication. However, currently available methods to evaluate casting stress or strain involve intrusive probes (which alter the casting solidification profile) or indirect estimation. Similarly, modelling of the mechanical response of a casting at the onset of hot tearing using computer simulation software remains difficult because of incomplete knowledge of a material's thermo-mechanical response at elevated temperatures. As a result, prediction of the onset of hot tearing is hindered by the absence of accurate and quantitative data about the stress and strain levels required to trigger hot tearing.

In this research, a novel and non-intrusive approach to quantify casting solidification strains at the onset of hot tearing was investigated. Neutron diffraction strain mapping was used to measure the elastic strain levels associated with the onset of hot tearing in two magnesium alloys. The AZ91D and AE42 magnesium alloys exhibit unique castability and solidification behaviour. The AZ91D alloy with its ~ 170 °C freezing range is typically easy to cast. However,

Received 30 June 2009. Accepted 4 November 2009. Published on the NRC Research Press Web site at cjp.nrc.ca on 30 April 2010.

L. Bichler and C. Ravindran.[2] Centre for Near-net-shape Processing of Materials, Ryerson University, 350 Victoria St, Toronto, ON, M5B 2K3, Canada.
D. Sediako. Canadian Neutron Beam Centre – NRC, Chalk River, ON, K0J 1J0, Canada.

[1]Special issue on Neutron Scattering in Canada.
[2]Corresponding author (e-mail: rravindr@ryerson.ca).

 doi:10.1139/P09-106

Fig. 1. Permanent mold used to evaluate hot tearing susceptibility. Dimensions are in mm.

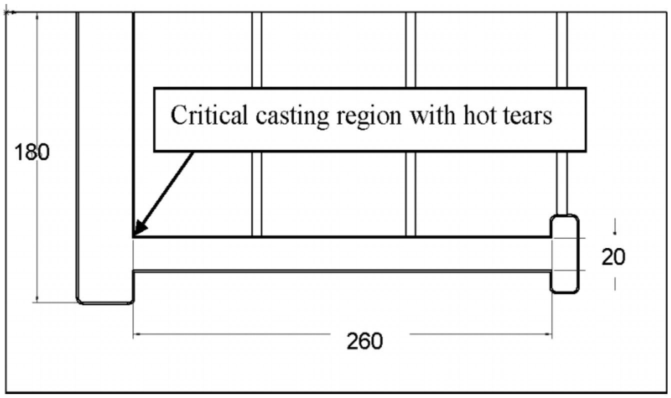

the long freezing range indicates that the alloy exists in a semi-solid stage for a long period of time. This may become important if dendrite coherency is reached at early stages of solidification, since subsequent interdendritic feeding becomes difficult and the formation of interdendritic shrinkage porosity and hot tears is likely. In the case of the AE42 alloy, which solidifies rapidly ($\sim$35 °C freezing range), only minimal shrinkage porosity is typically observed. However, the AE42 alloy contains numerous intermetallic compounds, which form above the liquidus temperature of α–Mg (625 °C). These intermetallic compounds segregate at the solidifying metal front and in the interdendritic regions. As a result, the hard and brittle intermetallics may decrease the AE42's ductility and increase its susceptibility to hot tearing. The difference in the magnitude of the freezing range of the two alloys also affects the rate of fraction of solids development driven by evolution of temperature gradients in the solidifying casting. In the permanent mold casting process, significant thermal gradients develop near the mold wall, resulting in concomitant evolution of fraction of solid gradients. Thus, in the AE42 alloy, significant thermal strain gradients may also contribute to the initiation of material failure. As a result, it was of interest to study and quantify the strain in AZ91D and AE42 castings associated with the onset of hot tearing in the two industrially relevant alloys.

2. Experimental procedure

To determine the casting process parameters corresponding to the onset of hot tearing, a series of trial and error experiments were performed. The objective was to manipulate the pouring and mold temperatures to produce castings with distinct degrees of hot tearing. For experiments with the AZ91D alloy, pouring temperatures from 680–720 °C and mold temperatures from 140–395 °C were investigated. In the case of the AE42 alloy, pouring temperatures below 720 °C resulted in the formation of hot tears for the entire available mold temperature range (room temperature to 395 °C). Therefore, the pouring temperature was systematically increased to reduce the casting cooling rate and prevent formation of hot tears. Castings were made at pouring temperatures of 720, 740, 760, and 765 °C and various mold temperatures.

The H-13 steel mold used in the experiments consisted of a downsprue and a 260 mm long horizontal bar with an end restraint, as shown in Fig. 1. The horizontal bar's cross section was 20 mm × 20 mm. The composition of the AZ91D and AE42 alloys was verified with an emission spectrometer and is provided in Tables 1 and 2, respectively.

These systematic experiments demonstrated that the onset of hot tearing for the AZ91D alloy occurred at 720 °C pouring temperature and between 210 °C and 250 °C mold temperatures. In the case of the AE42 alloy, the onset of hot tearing occurred at 765 °C pouring temperature and mold temperatures between 340 and 390 °C. When hot tears formed, they were located near the 90° corner in the proximity of the junction of the horizontal bar and the downsprue, as illustrated in Fig. 2. For the four casting conditions at the onset of hot tearing, three castings were produced at each mold temperature to verify repeatability of the hot tear severity.

Neutron diffraction (ND) strain mapping was performed at the Canadian Neutron Beam Centre in Chalk River, Canada. Elastic residual strain was measured along four linescans, as illustrated in Fig. 3. The experiments were carried out with a monochromatic beam of neutrons (λ = 2.371 Å), and a first-order diffraction (n = 1) analysis was performed. Using Bragg's law, the lattice spacing, d_{hkl}, of the crystallographic planes of interest at a given location was determined. The (hkl) planes of interest were the prismatic (100), basal (001), and two pyramidal (101) and (102) planes. A reference stress-free sample was obtained from the downsprue of the casting. The downsprue was free to contract (under very slow cooling) and thus contained minimal residual strain. Further, by machining the stress-free sample to 3 mm × 3 mm × 20 mm size, remaining residual strains were relieved. Using this sample, the stress-free lattice spacing $d_{o\text{-}hkl}$ was determined. The elastic lattice strain ϵ_{hkl} was calculated using the peak-shift method.

3. Results and discussion

Residual strain in the x-direction (ϵ_x) was seen to play a significant role on the evolution of hot tears in the critical regions of both alloy castings. Evolution of ϵ_x was the result of the axial contraction of the horizontal bar between the anchor and the downsprue. The development of ϵ_y and ϵ_z was discussed elsewhere [7]. Also, the determination of residual stresses using residual strains has been reported earlier [8, 9]. This paper focuses on a comprehensive comparison of strain evolution in two industrially relevant magnesium alloys at the onset of hot tearing.

3.1 AZ91D casting at 210 °C mold temperature

The ND measurements indicate that significant tensile residual strain developed for the (100) and (001) reflections, as observed in Fig. 4. In the case of the pyramidal (101) and (102) reflections, mixed strain values were observed.

These later two reflections exhibited a significant strain discontinuity in the critical region (–10 < x < 10 mm), as illustrated in Fig. 5a. For all three horizontal linescans (i.e., top edge, centerline, and bottom edge), tensile strain was observed in the downsprue (x < 0 mm) for (101) and (102) reflections. The tensile ϵ_x was relieved near the 90° corner. The relaxation of ϵ_x at this location was likely the result of

Table 1. Composition of AZ91D alloy (wt%).

Mg	Al	Zn	Mn	Si	Cu	Fe	Ni	Be
90.53	8.61	0.60	0.23	0.017	0.003	0.0038	0.0014	0.0012

Table 2. Composition of AE42 alloy (wt%).

Mg	Zn	Al	Cu	Mn	Ni	Be	Ce	La	Nd	Pr
93.69	0.01	3.65	0.002	0.36	0.0002	0.0006	1.3875	0.6858	0.4301	0.1407

Fig. 2. Hot tears forming at 90° corners of the junction between the horizontal bar and the downsprue (AZ91D alloy, 720 °C pouring temperature, 180 °C mold temperature).

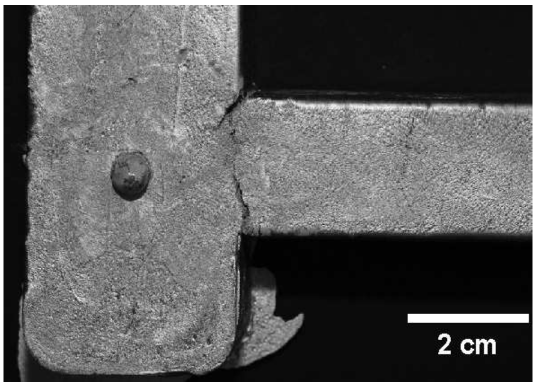

Fig. 3. Location of linescans.

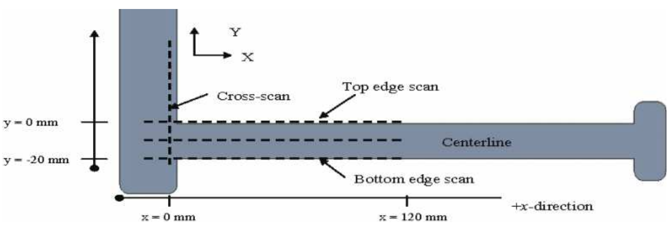

Fig. 4. Average strain and strain variance for AZ91D casting at 210 °C mold temperature.

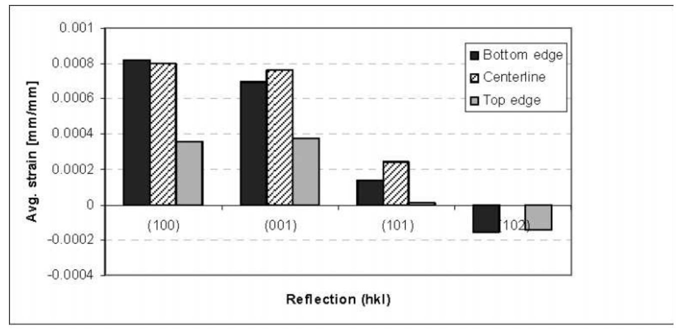

(a) Average strain.

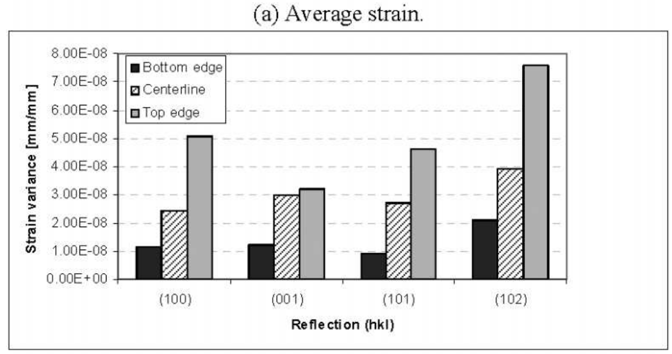

(b) Strain variance.

plastic damage associated with porosity formation or hot tearing.

The average strain values for the three linescans provide information about the general deformation of the horizontal bar during solidification. The bottom edge of the horizontal bar was in relative tension with respect to the top edge of the horizontal bar. This result was related to the expected filling sequence of the horizontal bar: the bar filled from the bottom edge upwards, with the top edge being the last area to fill. During filling of the horizontal bar, the alloy in contact with the relatively cool mold at the bottom edge started to solidify and formed a thin skin. As the bottom edge skin cooled, it began to contract. As it contracted, it compressed adjacent centerline regions of the casting. To maintain force equilibrium, the centerline regions resisted the compression of the bottom edge and thereby induced tensile strain in the bottom edge. This process repeated again for the solidifying centerline region and the top edge. As a result, the bottom edge developed relatively highest tensile strain. In contrast, the top edge of the horizontal bar was the last area to solidify and was allowed to deform the longest, thus locally relieving some of the developing residual strains. Further, observing the strain variance also suggests that the top edge of the horizontal bar solidified with high strain variation (i.e., strain gradients) in comparison with the centerline or bottom edge, which is also in agreement with the expected mold filling profile.

Observing the ϵ_x profiles for the bottom edge in Fig. 5*b*, it was noted that only a minor discontinuity in strain magnitude was observed near the bottom edge 90° corner (in comparison with the top edge profile in Fig. 5*a*). The improved strain homogeneity along the bottom edge suggests that the unrestrained contraction of the bottom portion of the downsprue (i.e., below the horizontal bar) possibly reduced the effect of the strain concentration at the bottom 90° corner. In contrast, the strains near the top edge 90° corner were intensified by the restrained axial contraction of the downsprue between the horizontal bar and a pouring cup located on top of the downsprue.

The strain intensification at the top edge 90° corner was examined in detail using strain measurements along the downsprue cross-scan. The ϵ_x profile in Fig. 6 shows that significant tension evolved in the sprue, and that axial contraction of the horizontal bar influenced material deformation well into the downsprue. Further, it was observed that the effect of *x*-direction contraction of the horizontal bar was not symmetrical across the $-20 < y < 0$ mm region. As

Fig. 5. ϵ_x profile for top and bottom edge linescans. Reflection: (102).

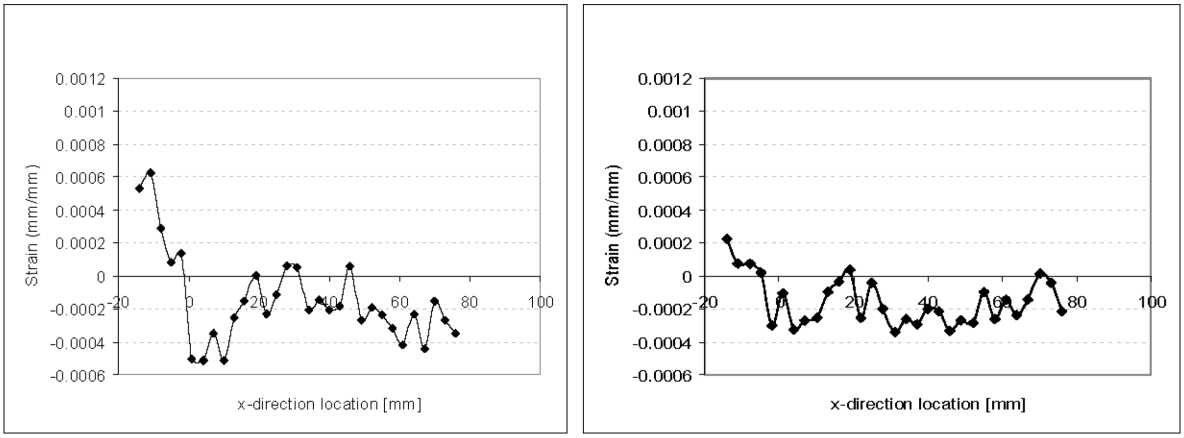

(a) Top edge. (b) Bottom edge.

Fig. 6. ϵ_x profile for (101) sprue cross-scan in AZ91D casting at 210 °C mold temperature.

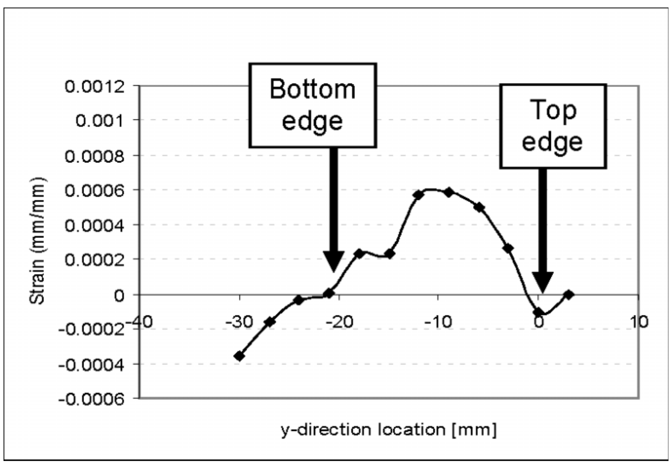

Fig. 7. Average strain and strain variance for AZ91D casting at 250 °C mold temperature.

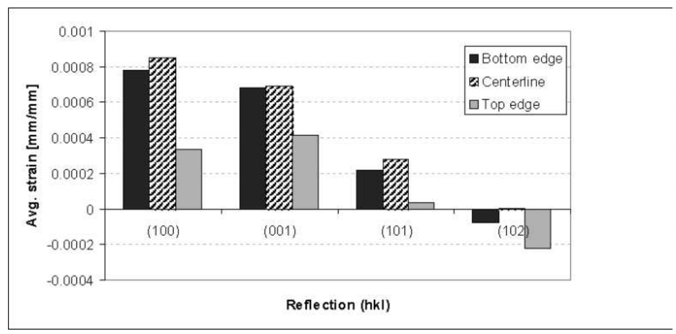

(a) Average strain.

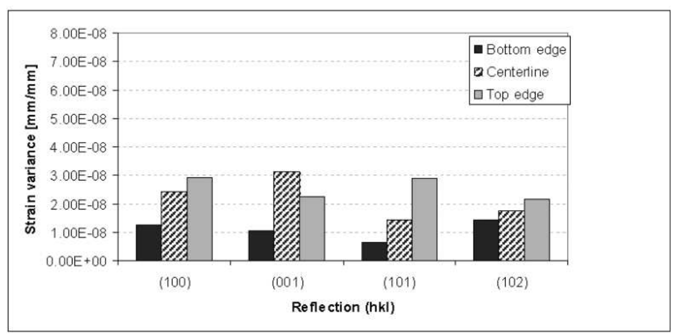

(b) Strain variance.

can be observed in Fig. 6, the tensile peak of the strain profile shifted towards the top edge corner. This shift was likely promoted by the free contraction of the bottom trap of the downsprue (resulting in relaxation of strain near the bottom edge 90° corner). Thus, it follows that the top edge 90° corner was highly susceptible to nucleate hot tears. These measurements are supported by empirical observation of hot tears on the castings.

Analysis of the average strain values for individual crystallographic reflections revealed additional information about the deformation of the matrix HCP crystals. It can be shown that a tension for (001) planes (c-axis extension) should result in (100) compression and (101) and (102) tension. Observing the results in Fig. 4, tension for the (001) basal planes did not result in compression of (100) or (101) planes, suggesting that plastic crystal deformation possibly occurred. As porosity formation and hot tearing are associated with plastic material deformation, it is thus possible that formation of these defects may have dissipated some of the strain energy of the HCP crystals.

3.2 AZ91D casting at 250 °C mold temperature

Analysis of the results revealed that increasing the mold temperature from 210 to 250 °C resulted in only a marginal decrease of the average ϵ_x residual strain, but in a significant decrease of the strain variance (especially along the top edge), as observed in Fig. 7. This observation indicates that both castings (210 and 250 °C mold temperatures) had to contract by approximately the same amount during cooling to room temperature; thus, their bulk (total) average strain was similar. However, increasing the mold temperature homogenized the temperature and strain distribution, resulting in the reduction of ϵ_x strain gradients along the horizontal bar.

The decrease of strain gradients was particularly evident for the (101) and (102) reflections, as illustrated in Fig. 8. In the case of a casting with a hot tear, the ϵ_x strain in the

Fig. 8. ϵ_x profile for (101) top edge linescan in AZ91D castings.

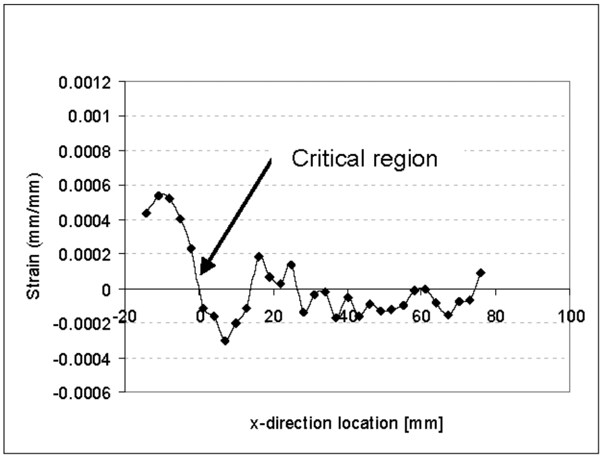

(a) 210 °C mold temperature.

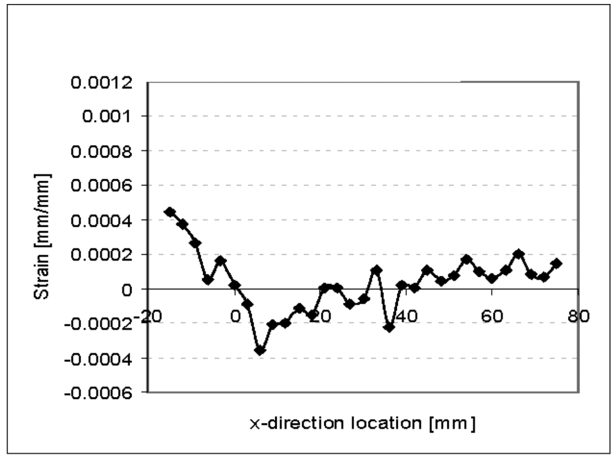

(b) 250 °C mold temperature.

Fig. 9. Average strain and strain variance for AE42 casting at 340 °C mold temperature.

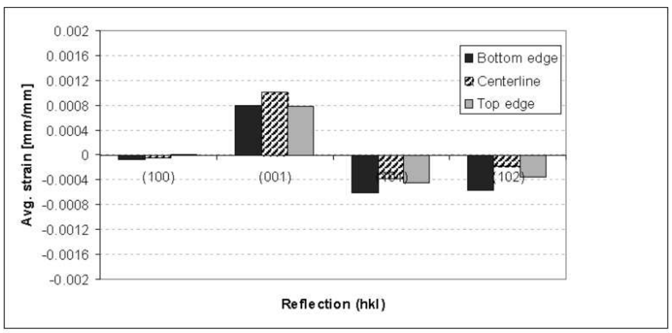

(a) Average strain.

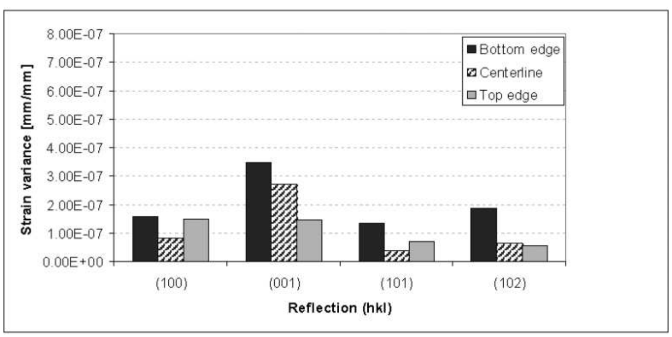

(b) Strain variance.

sprue region was 0.000 514 mm/mm (tensile). Strains were relieved in the area of the crack, as indicated by a drop in the strain profile in Fig. 8*a*. The ϵ_x in the horizontal bar to right of the 90° junction was tensile 0.000 182 mm/mm (locations: 15–20 mm). In the case of a casting without a hot tear, the ϵ_x strain in the downsprue was also tensile 0.000 441 mm/mm. However, contrary to the cracked casting, the region to the right of the 90° junction possessed compressive ϵ_x strain of 0.000 113 mm/mm. The strains in the 250 °C mold temperature casting became tensile only far away from the 90° junction.

This difference in the ϵ_x strain profile at the top edge 90° corner was related to the feeding of the casting. At high mold temperatures, interdendritic liquid feeding was possible for a longer period of time. Thus, the axial contraction of the horizontal bar was compensated by incoming liquid metal feed from the downsprue, and the developing strains were continuously alleviated. However, for the low mold temperature casting, the horizontal bar solidified and contracted without adequate compensation by liquid metal, and tensile strains developed. Increasing the mold temperature decreased the strain gradients and made the casting deformation more homogeneous. These factors, along with directional solidification, likely decreased formation of local stress concentrations along the horizontal bar and decreased the susceptibility of the 250 °C mold temperature casting to initiate hot tears.

3.3 AE42 casting at 340 °C mold temperature

The average strain and variance values for the AE42 casting made at 340 °C mold temperature are presented in Fig. 9. Unlike the case of the AZ91D castings, evolution of significant tensile or compressive strains along the horizontal bar (i.e., in the *x*-direction) was not observed, as Fig. 10*a* illustrates. In particular, the strain in the critical region did not show elevated tension or relaxation at the 90° corners, as was observed in the AZ91D castings (e.g., Fig. 8). The reduced effect of axial contraction was further confirmed by analyzing the sprue cross-scan results in Fig. 10*b*. There was only minimal increase of ϵ_x in the critical region $-20 < y < 0$ mm. Thus, possibly due to the fast solidification of the AE42 alloy, complex residual strain profiles did not have sufficient time to develop.

Observing the average strain values in Fig. 9*a*, reflections (100), (101), and (102) evolved compressive residual strain, while basal (001) planes carried significant tensile strain. Thus, plastic deformation of the HCP crystal occurred, similarly as in the case of AZ91D castings.

The strain variance results in Fig. 9*b* suggest that the bottom edge of the casting had elevated strain non-uniformity in comparison with the centerline or top edge. Evolution of the strain gradients along the bottom edge was possibly related to the rapid solidification of the alloy upon contact with the mold (i.e., presence of a thermal shock). Melt temperature variation during mold filling of the bottom edge in

Fig. 10. ϵ_x profile for (101) reflection for AE42 casting at 340 °C mold temperature.

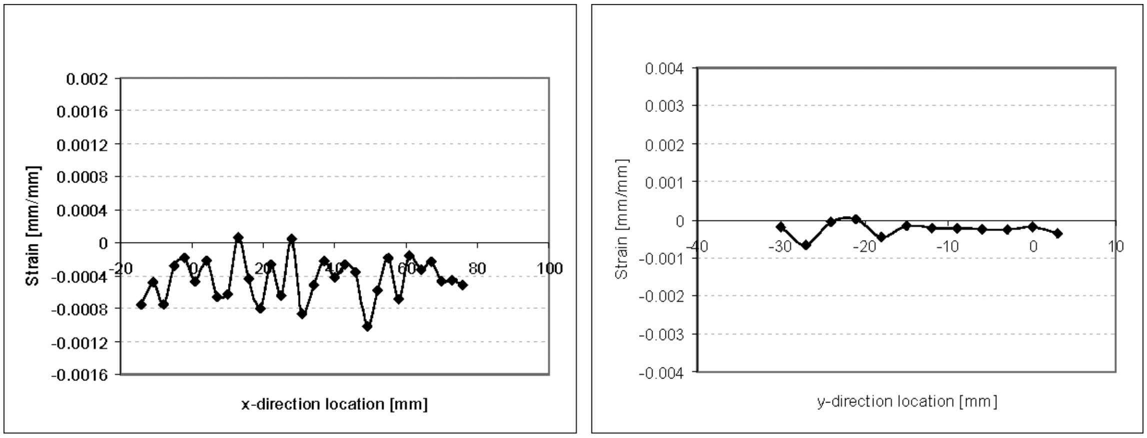

(a) Top edge scan. (b) Sprue cross-scan.

Fig. 11. Average strain and strain variance for AE42 casting at 390 °C mold temperature.

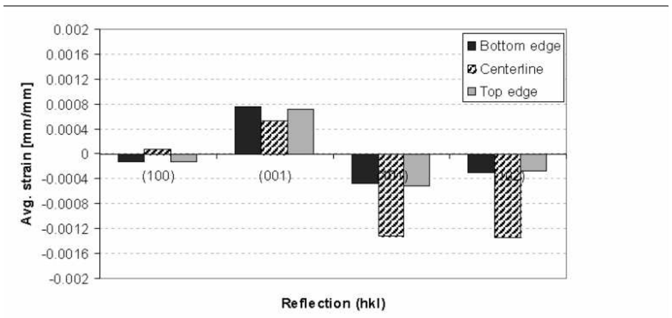

(a) Average strain.

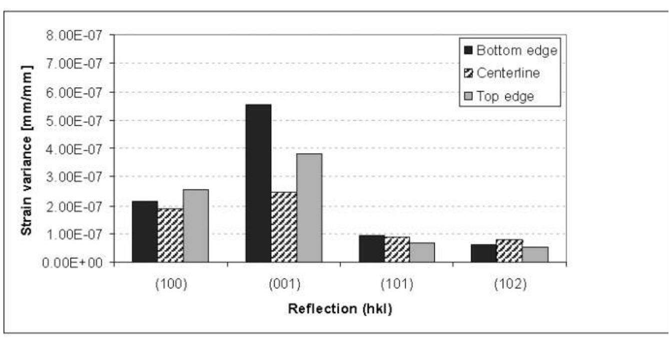

(b) Strain variance.

conjunction with the short freezing range of the alloy resulted in inhomogeneous fraction of solids and strain gradient evolution. Comparing the magnitude of the ϵ_x strain variance in Fig. 9*b* with that of the AZ91D alloy (e.g., Fig, 4*b* or Fig. 7*b*), it is apparent that the AE42 alloy solidified more uniformly. That is, because of the rapid hoop solidification of the AE42 casting, axial ϵ_x strain profiles did not have sufficient time to develop.

3.4 AE42 casting at 390 °C mold temperature

The average strain and strain variance results are presented in Fig. 11. Comparison of Fig. 9*a* and Fig. 11*a* reveals that increasing the mold temperature marginally decreased the ϵ_x tension in the horizontal bar of the 390 °C mold temperature casting. This trend was expected, as slower casting solidification enabled interdendritic liquid feeding to accommodate solidification shrinkage, resulting in a decrease of residual strain. Specifically, comparing Fig. 9 with Fig. 11, it appears that the (001) tension decreased when the mold temperature increased. Considering the average strain for the entire horizontal bar's cross-section (i.e., including bottom edge, centerline, and top edge), increasing the mold temperature decreased the average strain from 8.56×10^{-7} mm/mm to 6.66×10^{-7} mm/mm, a 28.5% decrease.

Fig. 11*b* suggests that with slower casting solidification, the material was allowed to develop localized axial strain gradients, which resulted in increased axial strain variance in comparison with the 340 °C casting. This trend was unique to the AE42 alloy and was contrary to that observed for the AZ91D alloy.

Similarly, as in the case of a casting made at 340 °C mold temperature, the cross-scan in the downsprue did not indicate a significant variation in the critical region (i.e., $-20 < y < 0$ mm). Thus in general, the effect of the horizontal bar's axial contraction did not extend deep into the downsprue.

The effect of linear thermal contraction on the residual strains measured with ND was also examined. A detailed analysis is presented elsewhere [7]. The results indicate that cooling of the casting from the solidus temperature to the room temperature (at which ND was performed) possibly introduced a maximum measurement error in the reported strain values of $\sim 11\%$. This maximum error was deemed acceptable and the reported ND results provide meaningful information previously unavailable.

4. Conclusions

The results of this study indicate that the hot tearing susceptibility of permanent mold cast AZ91D and AE42 magnesium alloys can be manipulated by suitably adjusting the mold temperature. For an AZ91D alloy poured at 720 °C, the onset of hot tearing occurred between 210 and 250 °C mold temperatures. For an AE42 alloy poured at 765 °C, the onset of hot tearing occurred between 340 and 390 °C mold temperatures.

The fundamental mechanisms associated with the onset of hot tearing in the two magnesium alloys were identified as follows.

4.1 AZ91D alloy

Nucleation of microcracks occurred at a stress concentration (90° corners of the junction of the horizontal bar and the downsprue). Thermal contraction of the casting and evolution of shrinkage porosity increased the tensile strain in the critical region. This tensile strain increased the local strain condition beyond the yield strength of the semisolid alloy. Subsequently, formation of shrinkage porosity was followed by the nucleation and propagation of a hot tear. As the mold temperature increased, the size of the interdendritic feeding paths increased and long-range interdendritic feeding of the casting improved. Thus, feeding compensated the casting's volumetric contraction and decreased the magnitude of tensile strains in the critical region of the casting.

Development of tensile ϵ_x strain along the horizontal bar was measured with ND for both AZ91D castings. The ϵ_y and ϵ_z strains remained compressive. The magnitude of the tensile ϵ_x strain only marginally decreased with an increase of the mold temperature. The increase of the mold temperature, however, significantly improved strain homogeneity in the critical region, thereby reducing the detrimental effect of the 90° stress concentration on material failure. As a result, the susceptibility to hot tearing in the AZ91D alloy decreased with increasing mold temperature.

4.2 AE42 alloy

Hot tears nucleated at the 90° corners of the casting and propagated in the direction of the maximum stress gradient. When hot tears formed, the tensile strain at the 90° corner reached 0.0009 mm/mm. As the mold temperature increased, the permeability of the interdendritic regions improved. As a result, the tensile residual strain decreased to 0.0007 mm/mm. In the AE42 alloy, shrinkage porosity was not observed to play a fundamental role on hot tearing. Instead, the rate of solidification shrinkage and thermal contraction appeared to influence formation of hot tears.

Acknowledgements

The authors would like to acknowledge the financial support of the Natural Sciences and Engineering Research Council (NSERC) of Canada. One of the authors (LB) is grateful for the award of a NSERC-Canada Graduate Scholarship. The authors would also like to thank Mr. I. Kosi of Meridian Technologies for the provision of materials and Mr. A. Machin of Ryerson University for technical assistance.

References

1. C. Monroe and C. Beckermann. Mater. Sci. Eng. A, **413–414**, 30 (2005). doi:10.1016/j.msea.2005.09.047.
2. D.G. Eskin and L. Katgerman. Prog. Mater. Sci. **49**, 629 (2004). doi:10.1016/S0079-6425(03)00037-9.
3. N. Hort, H. Dieringa, and K.U. Kainer. Trans. Indian Inst. Met. **58**, 703 (2005).
4. Y. Wang, B. Sun, Q. Wang, Y. Zhu, and W. Ding. Mater. Lett. **53**, 35 (2002). doi:10.1016/S0167-577X(01)00449-9.
5. G.K. Sigworth. AFS Trans. **104**, 1053 (1996).
6. M. Rappaz, J.M. Drezet, and M. Gremaud. Metallurg. Mat. Trans. A, **30**, 449 (1999). doi:10.1007/s11661-999-0334-z.
7. L. Bichler. Ph.D. Thesis, Ryerson University. 2009.
8. L. Bichler, C. Ravindran, and D. Sediako. Can. Metallurg. Quart. **48**, 81 (2009).
9. L. Bichler, C. Ravindran, and D. Sediako. Trans. Indian Inst. Met. **61**, 293 (2008).